Chapter 4

Aluminum Anodic Oxide AAO as a Template for Formation of Metal Nanostructures

Piotr Tomassi and Zofia Buczko

Additional information is available at the end of the chapter

http://dx.doi.org/10.5772/61263

Abstract

The aim of the chapter is to describe the applications of AAO as a template in metal nanostructures formation and to present the experimental results obtained by authors in this field. The basic mechanism of the process of anodic oxidation of aluminum was described. The influence of oxidation parameters on the AAO structure was discussed. The processes of electrochemical metal deposition in AAO were described. The main present as well as future applications of metal nanostructures formed were listed.

Keywords: anodic oxidation of aluminum (AAO), metal nanostructures

1. Introduction

The aim of this chapter is to describe the applications of AAO as a template in metal nanostructures formation and to present the experimental results obtained by authors in this field.

Metals in a state of high dispersion currently play an important role in technology. Their chemical and physical macroscopic properties, such as the rate of their reaction with other substances, colours and mechanical properties are significantly different from the bulk metals. Fundamental research and technology development over the last decade have resulted in wider use and implementation of metal-containing materials in a state of high dispersion into the industrial practice.

Solid nanoparticles are a system of unstable thermodynamic state, so even precious metals are not found in this form in nature. However, in the case of metals having a high cohesive energy, and thus a high melting point, it is possible to obtain and maintain them in the form of nanodispersion for a long period of time. This is the case of high activation energy of the

agglomeration process of particles, which is a crucial parameter. This applies in particular to transition metals. Nanodispersions of these metals are most often applied in practice.

The basic properties of highly dispersed metals are described in monographs of Romanowski [1] and also of Feldheim and Foss [2]. The authors point out that the systems containing metal nanoparticles are particularly interesting because their synthesis and chemical modification are simple. The main directions, according to the authors, of current basic research are given in the following text.

1.1. Investigation of optical properties

Metal particles often exhibit strong plasmon resonance extinction bands in the visible spectrum. While the spectra of molecules can be understood only in terms of quantum mechanics, the plasmon resonance bands of nanoscopic metal particles can often be described in terms of classical free-electron theory and electrostatic models for particle polarizability. In contrast to molecular systems, the linear optical properties of metal nanoparticle composites can be changed significantly without a change in essential chemical composition.

Optical properties of metal nanoparticles are usually described by Mia theory. Material testing is mostly done by optical spectroscopy. Deviation from the theoretical and measured values is unavoidable due to uneven sizes and shapes of metal particles in real systems and the diversity of their distribution in a material. Therefore, theoretical analytical methods are not enough to describe the real particle systems and numerical methods are often implemented. Investigation results of extinction, absorption, scattering, and optical interaction of metal nanoparticles can be found, among others, in the work of Lin et al. [3] and Noguez et al. [4].

1.2. Investigation of electrical properties

Metal particles and bulk materials are similar taking into account their electrical properties. Simple classical charging expressions and RC equivalent circuit diagrams can be used in both cases to describe surface charging and electron transport processes. Description of electric properties of metal nanoparticles requires knowledge of their size and dielectric properties of the surrounding medium.

Examples of research in this field are given in the work of Wu et al. [5] on study of metal clusters of silver, gold, and copper. Static electric polarizability and absorption spectrum have been measured. Density functional theory (DFT) has been implemented for description of investigated systems. A competition of charge transfer and electron cloud distortion was proposed for explaining the spacing dependence of both electric and optical properties.

1.3. Investigation of magnetic properties

Small, single-domain ferromagnetic particles, containing a few tens or a few hundred atoms have a large total magnetic moment. When these ferromagnetic particles are separated by comparatively large distances, their magnetic moments do not interact strongly and they form a system of magnetic dipoles, whose relative orientation can be randomized by thermal motion

http://dx.doi.org/10.5772/61263

even in relatively low temperatures. The overall magnetization of the system is therefore similar to that of a paramagnetic material, expressed by the Langevin equation.

The study of ferromagnetic nanoparticles systems are mainly targeted to the specific use of new nanomaterials. In particular, researches are provided to receive improved materials for high-density data storage, for the construction of high-speed computing components, and for a new-generation high-performance display.

The test results of the magnetic properties of metal nanoparticles have been published, among others, by Kim et al. [6]. The authors investigated Ni-Co, Ni-Fe, and Co-Pt alloy nanoparticles. Magnetic hysteresis loops were presented and values of magnetic susceptibility, the saturation magnetization, and coercivity were calculated.

Implementation of porous alumina, obtained by anodic oxidation of aluminum, as a template for producing new nanostructured materials is a quickly developing part of nanotechnology in recent years. Introducing a metal by electrodeposition inside the AAO pores, it is possible to obtain a durable material, characterized by a uniform structure of nanoparticles of a single metal or alloy in a matrix of dielectric amorphous alumina. The basis of manufacturing processes of composite materials of this type is presented in the following sections. References are listed in Table 1.

No.	Subject	References
1.	Basic properties of highly dispersed metals	[1, 2]
2.	Optical properties of metal particles	[3, 4]
3.	Electrical properties of metal particles	[5]
4.	Magnetic properties of metal particles	[6]
5.	The theories of anodic oxidation of aluminum	[7–12]
6.	Theoretical modeling of porous oxide growth on aluminum	[13–19]
7.	Preparation of AAO as a template in nanotechnology	[20–48]
8.	The processes of metal electrodeposition on AAO template	[49–68]

Table 1. Basic studies on AAO as a template for formation of metal nanostructures

2. Anodic oxidation of aluminum

Passivation phenomenon of aluminum spontaneously occurs in contact with oxygen and thin film of alumina on the surface of the metal is formed. Thicker oxide coatings can be produced by the use of electrochemical anodic polarization in selected solutions. This surface finishing of aluminum work pieces is widely applied for corrosion and abrasion protection and for decorative purposes.

In carrying out the anodizing process of aluminum in an electrolyte, which slightly dissolves alumina, an oxide layer is formed with a unique porous structure on the metal surface. Highly

ordered pores are perpendicular to the base and pass through almost the entire thickness of the oxide layer. Directly on the metal surface nonporous barrier layer is grown and it usually has a thickness of several tens of nanometers. When an aluminum substrate with high purity and uniform structure is used and the parameters of the operation of the electrochemical oxidation are carefully controlled, homogeneous distribution of pores as a hexagonal network can be obtained. The pore diameters are uniform; it depends on the oxidation conditions and can be controlled in the range from 10 to several hundred nanometers. The total thickness of the oxide layer is determined by the oxidation time. It is usually in the range of tenths of a micron to tens of microns. The schematic drawing of the AAO structure is presented in Figure 1.

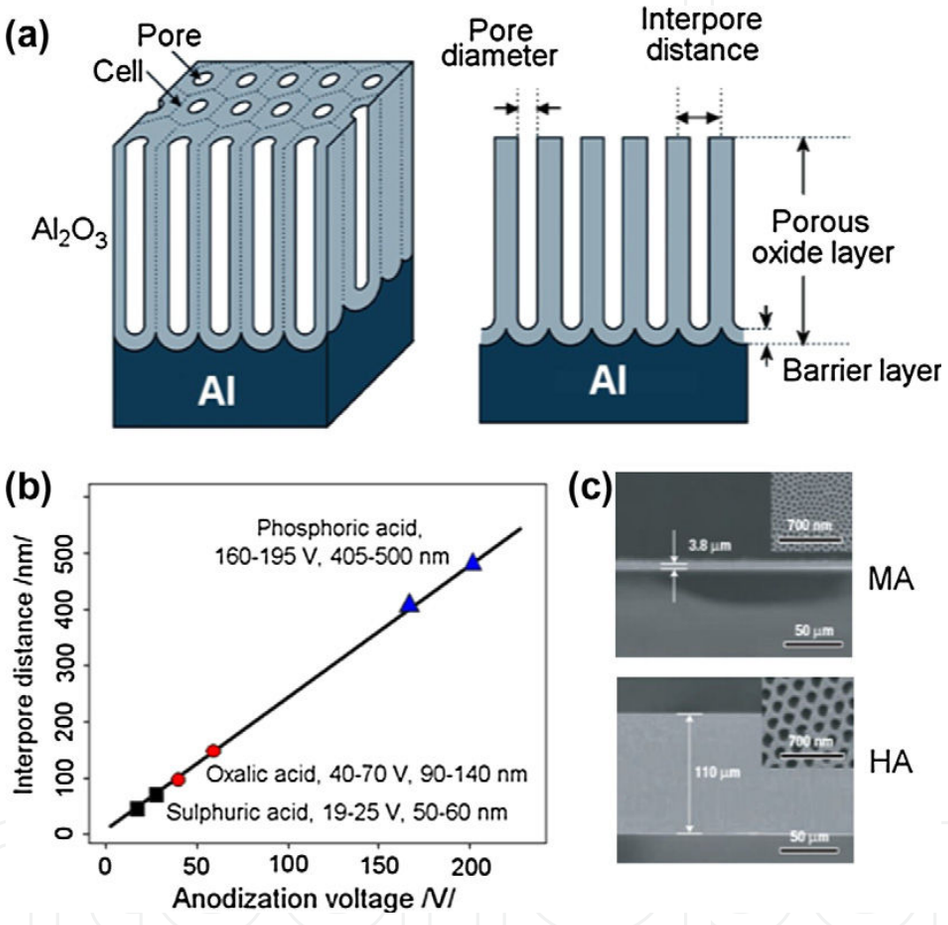

Figure 1. (a) Schematic drawing of AAO structure prepared by electrochemical oxidation of Al. (b) Summary of self-ordering voltage and corresponding interpore distance of AAO produced within three well-known regimes of electrolytes (sulfuric, oxalic, and phosphoric). (c) (Top) SEM cross-sectional view of AAO membrane formed by MA (0.3 M $H_2C_2O_4$, 1°C, 40 V) and (bottom) by HA (at 140 V) for 2 h (insets: SEM top view of pore structures). Permission Elsevier [61].

The mechanism of the process of anodic oxidation of aluminum and forming the porous oxide layer is still under investigation. There are some basic theories, like the Keller, Hunter, and Robinson geometric model [7] and the colloidal one of Murphy and Michelson [8]. It is believed that the porous structure is a result of two competitive reactions: Al_2O_3 forming and dissolution of the oxide. These reactions are stimulated by the electric field that is distributed inside the

http://dx.doi.org/10.5772/61263

barrier layer. The electric field intensity inside the barrier layer is of the order of 1 V/nm during the oxidation process. Such high field is needed to excite the ionic current inside the oxide. This field also stimulates the dissolution reaction ("field-assisted dissolution"). Also, due to the tunneling effect, additional electron current may occur. The role of that current in the anodic oxidation of aluminum was described by Palibroda [9-10].

A summary of recent interpretations of the reaction mechanism of anodic oxidation of aluminum can be found in the Brace monograph [11] and the Wielage et al. work [12]. The total chemical reaction is as follows:

$$2Al + 3H_2O \rightarrow Al_2O_3 + 6H^+ + 6e^- \quad (1)$$

It consists of two partial reactions:

$$2Al \rightarrow 2Al^{3+} + 6e^- \quad (2)$$

$$3H_2O \rightarrow 6H^+ + 3O^{2-} \quad (3)$$

The oxide forms due to migration of Al^{3+} ions from basic metal into the solution, while the movement of ions O^{2-} is in the opposite direction. Under the influence of a high electric field, there is ionic conductivity in the oxide layer where the aluminum and oxygen ions are charge carriers.

A characteristic porous structure of the alumina layer is formed as a result of the chemical and electrochemical dissolution of the oxide. Dissolution reaction is promoted by local increase in hydrogen ion concentration (reaction 1) and high electric field inside the barrier layer ("field-assisted dissolution"). Due to the high electrical resistance of the barrier layer, the Joule heat is given off during a flow of electric charge, which causes local increase in temperature and also enhances the dissolution reaction of the oxide.

Defects and impurities, which are always present in the metal substrate, are precursors of pores. Due to the contact with an aqueous solution to the oxide layer surface, there are always various intermediate forms of hydrated oxide, including aluminum hydroxide. In addition, due to the adsorption of anions from the solution, the oxide material is enriched with other compounds, like for example sulfates in the case of processing in sulfuric acid.

Oxide layer with porous structure is obtained using solutions of dibasic and tribasic acids, in which the oxide is dissolved. When the critical thickness of the barrier layer is obtained, pores are initiated in flows, cracks, and impurities spots. Only some part of embryo pores develops up to form final porous structure with the hexagonal arrangement. It is determined by the reactions' activation energy of oxide formation and dissolution, also by the distribution of electric field in the barrier layer

Attempts have been made to create modeling and mathematical description of the electrochemical processes of formation of porous aluminum oxide layers [13-18]. Parkhutik and Shershulsky [13] are the first to prove that the potential distribution inside the oxide layer can be calculated with the use of Laplace equation. Calculations with the adequate assumptions of the local moving rate of the solution–oxide and oxide–metal phase boundaries have been made for a number of cases in the two-dimensional system. As the results pictures of the development of porous structures have been obtained similar to those observed on the SEM images of experimental samples. Also, numerical approximations are often used for the mathematical modeling [19].

Beside the above-described mechanism of aluminum anodic oxidation process and its mathematical modeling, the authors point to additional important factors that have an impact on the process of forming a porous oxide structure:

1. The volume of the oxide is higher than the metal consumed and therefore there are strong strains in oxide layer that cause mechanical stress fractures (cracks). These cracks are often the beginning of a pore.
2. The process of oxidation may be affected by local differences in the wettability of the surface of the oxide.
3. Part of the aluminum ions Al^{3+} is ejected from the metal to the solution without binding to the oxide structure. This phenomenon reduces the current efficiency of anodic oxidation reaction.
4. In the presence of phases containing foreign elements in aluminum substrate, it is possible, as polarization is anodic, side reaction of evolution of oxygen gas to occur. Like the previous phenomenon, it reduces the current efficiency of the oxidation reaction.
5. Barrier layer thickness, the distance between the pores and their diameters are proportional to the applied voltage, with the other process parameters being fixed.

On the basis of these assumptions, Wu et al. [17] attempted to demonstrate that the chemical and electrochemical reactions of oxide dissolution do not have significant effect on the process of forming a porous oxide structure. This statement, however, is not consistent with the conclusions of other authors.

3. Preparation of AAO template

A porous oxide coating can be obtained by anodic oxidation of aluminum using a number of different types of electrolyte solutions. Sulfuric, oxalic, phosphoric, or chromic acids solutions are typically implemented. The porous anodic layer can also be obtained from solutions of many organic acids, especially the polybasic acids, such as tartaric, citric, sulfosalicylic, maleic, and succinic acids.

Such coating parameters as the thickness of the barrier layer, pore diameter, the distance between the pores and their surface density considerably vary depending on the type of

http://dx.doi.org/10.5772/61263

processing solutions, as is shown in Tables 2 and 3 [20]. For a given type of solution, the geometric parameters of the net of pores can be controlled by varying the voltage during anodic oxidation. The thickness of the barrier layer and the diameter of the pores are proportional to the applied voltage (Table 2). The pore diameter is usually from 10 to a few tens of nanometers. Pores having higher values of diameter can be obtained from solutions of phosphoric acid or organic acids at high voltages. Li et al. [21] give the equation that correlates distance between the pores and the voltage and pH value for processing solutions. Uniform grid of unusually high pore diameters of up to 200–500 nm have been successfully obtained with properly selected oxidation conditions in solutions containing phosphoric acid and/or organic acids with high voltage current in [22-26]. In the solution of citric acid using high current voltage, Mozalev et al. [27] obtained the interpore distance 1.1 μm, barrier layer thickness 0.5 μm, and pore diameter 0.23 μm. Also, lowering the temperature of anodic oxidation, thicker coatings can be easier to obtain; their porosity is lower and hardness is higher. The examples of SEM images of AAO coatings are presented in Figures 2 and 3.

Electrolyte	Conc. % (wt)	Temp. ^{O}C	Barrier layer thickness nm/volt	Pore diameter nm/volt	Wall thickness nm
Phosphoric acid	4	25	1.19	1.10	33
Oxalic acid	2	25	1.18	0.97	17
Chromic acid	3	40	1.25	1.09	24
Sulfuric acid	15	10	1.0	0.80	12

Table 2. Barrier characteristics for various electrolytes [20]

Electrolyte	Conc. % (wt)	Temp. $^{\circ}C$	Voltage, V	Pores per cm^2
Sulfuric acid	15	10	15	76×10^9
			20	52×10^9
			30	28×10^9
Oxalic acid	2	25	20	35×10^9
			40	11×10^9
			60	6×10^9
Chromic acid	3	50	20	22×10^9
			40	8×10^9
			60	4×10^9
Phosphoric acid	4	25	20	19×10^9
			40	8×10^9
			60	4×10^9

Table 3. Pore density in oxide coatings [20]

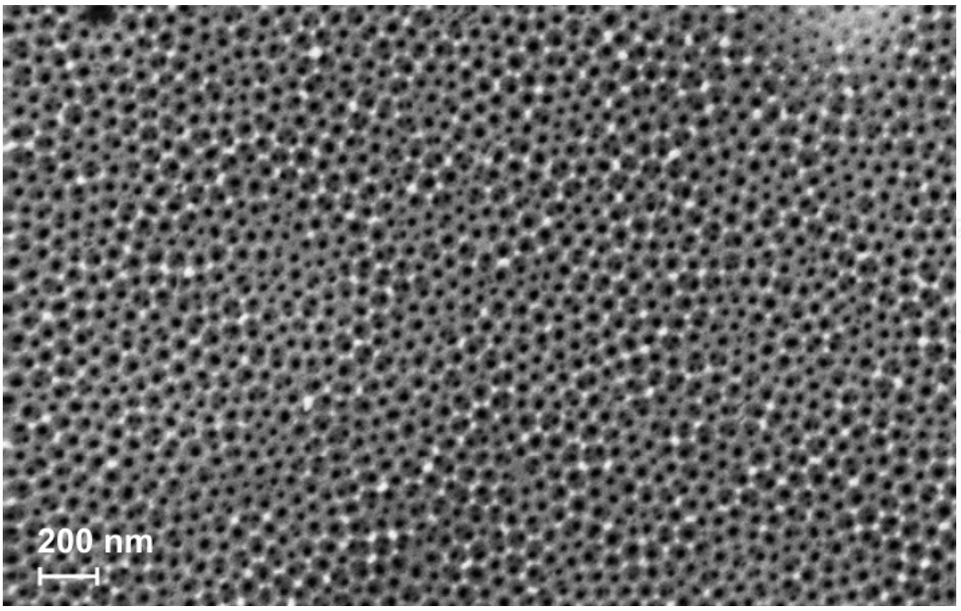

Figure 2. SEM image of AAO coating obtained in solution of sulfosalicylic acid 50 g/dm^3, oxalic acid 10 g/dm^3, and sulfuric acid 5 g/dm^3, 3 A/dm^2, 20^{O}C, 30 min. Permission Librant [114].

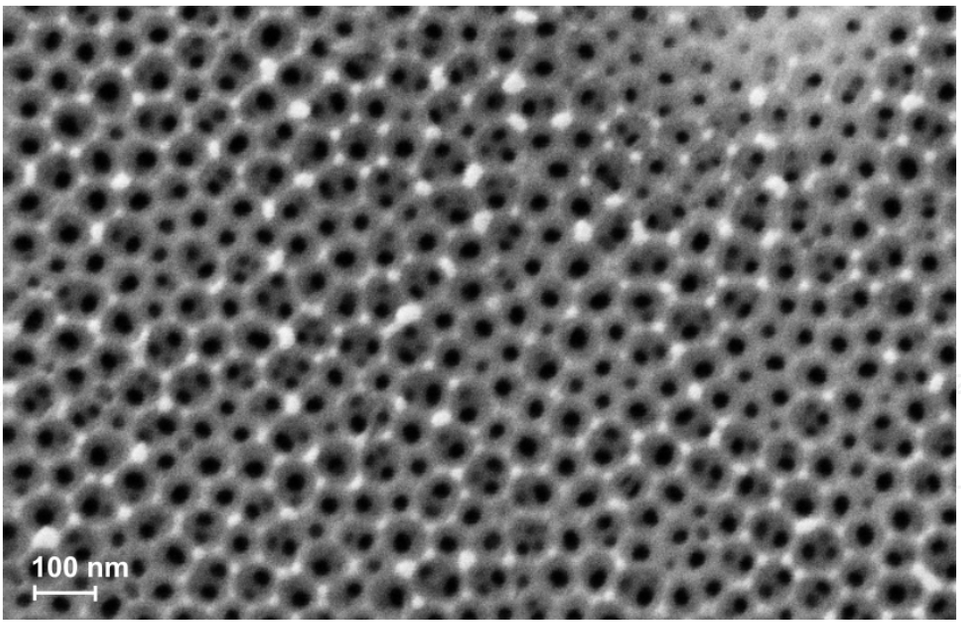

Figure 3. SEM image of AAO coating obtained in solution of sulfosalicylic acid 50 g/dm^3, oxalic acid 10 g/dm^3, and sulfuric acid 5 g/dm^3, 3 A/dm^2, 20^{O}C, 30 min. Permission Librant [114].

For many applications of Al_2O_3 coatings in nanotechnology, including membranes for nanofiltration, it is necessary to separate oxide layers from aluminum substrates. The following techniques are most frequently used:

http://dx.doi.org/10.5772/61263

1. Screening of a part of the electrode surface with lacquer. After anodizing, the lacquer coating is removed, and then the aluminum substrate is entirely dissolved using a solution that is not aggressive to the oxide, e.g., copper chloride solution containing hydrochloric acid [28], mercury chloride solution [29], or a saturated solution of iodine in methanol [30].

2. Programmable voltage reduction in the final stage of anodic oxidation. A thin oxide layer of high porosity and small pore wall thickness is created bottom-up from the substrate. The thickness of the nonporous barrier layer also tends to decrease. As a result, the mechanical properties of the bottom oxide layer are reduced and it can easily be separated from the substrate [31], sometimes in an additional operation of chemical or electrochemical dissolution. For this purpose, for example, Zhao et al. [32] used a cathodic polarization in a solution of potassium chloride.

For applications in nanotechnology, it is very important to obtain the pore distribution, which is homogeneous and uniform over the entire surface in the oxide layer. In order to obtain the highest possible uniformity of the pore distribution, the following techniques are applied:

1. The use of additives to the solutions usually in the form of aliphatic alcohols, glycerol, or ethylene glycol [22,32-35]. The addition of ethanol or methanol facilitates heat removal from the barrier layer during the process of oxidation and reduces the risk of defects in the oxide coating. It also allows the use of high current density, which significantly shortens the creation of oxide coating. Li et al. [36] achieved current density of 4000 A/m^2 during anodic oxidation process in solution phosphoric acid–ethanol.

2. Application of programmed pulse current instead of direct current [37-40]. Anodic and cathodic pulses are used alternately or only anode pulses with a break. According to the authors, the use of pulsed current allows for better structure uniformity of the oxide layer and reduces the risk of defects caused by heat generated in the barrier layer during the oxidation process.

3. The use of a two-step anodizing process. Today it is a commonly used technique which allows increasing the distribution uniformity of the pores and reduces the scatter of their geometrical parameters. Polished aluminum surface is anodically preoxidized. An oxide layer is selectively removed in a subsequent operation. Usually for this purpose the etching solution of phosphoric and chromic acids is used, which does not affect the aluminum substrate. After this operation, the aluminum surface has a scalloped structure, so the homogeneity of the oxide layer formed in the second stage of anodic oxidation increases [41-44].

4. The initial formation of the aluminum surface by mechanical, laser, or other method [45-47]. Zaraska et al. [45] listed the following surface-shaping techniques:

   - Prepatterning using a tip of the scanning probe microscope (SPM) or atomic force microscope (AFM)
   - Focused ion beam lithography
   - Holographic lithography

- Using stamps (molds) with regular array of convexes prepared lithographically
- Optical diffraction grating
- Nanosphere lithography (NSL)

Asoh et al. [46] obtained square layout of cells with centrally located pores after the initial shaping of a surface using the imprinting process. This square system is fundamentally different from the natural hexagonal distribution of pores.

Choi et al. [47] implemented a similar technique and got a uniform distribution of pores having a triangular cross section.

As can be seen there is a great range of possibilities of appropriate selection techniques for producing the porous aluminum oxide layer in order to achieve a certain distribution and pore geometry for use in nanotechnology. For example, a typical technique used to obtain a template for the production of metallic nanostructures is shown in Table 4 [29].

Various tools can be used for evaluation of the uniformity of pore distribution, e.g., Voronoi diagrams, radial distribution function (RDF) [48], fast Fourier transform (FFT) images, Delaunay triangulations (defects map), pair distribution functions (PDF), or angular distribution functions (ADF) [44].

Step no.	Process
1.	Degreasing of AA 1050 alloy in ethanol and acetone
2.	Electrochemical polishing Perchloric acid (60 wt.%) and ethanol (1:4 vol) Constant potential 20 V for 1 min at 10^{O}C
3.	Anodic oxidation in 0.3M oxalic acid Constant potential 45V for 60 min at 20^{O}C
4.	Alumina layer removal by chemical dissolution 6 wt.% H_3PO_4 + 1.8 wt. % $H_2Cr_2O_4$ Time 12 h, temperature 45^{O}C
5.	Anodic oxidation in 0.3M oxalic acid Constant potential 45V for 1, 2, 4, or 8 h at 20^{O}C The samples with different coating thicknesses were obtained
6.	Removal of aluminum substrate by chemical dissolution Saturated $HgCl_2$ solution
7.	Chemical etching of alumina barrier layer 5 wt.% H_3PO_4 at 25^{O}C

Table 4. The example of procedure of AAO template formation [29]

http://dx.doi.org/10.5772/61263

4. Metal deposition

The composite systems AAO–metal can be formed by inexpensive and simple method of electrochemical metal deposition. It does not require complex equipment as in the case of CVD or PVD methods.

The first attempts of metals electrodeposition inside the pores of the anodic oxide layer on aluminum AAO were associated with the development of electrochemical coloring technology. Metal nanoparticles can be deposited into the pores of Al_2O_3 layer by transferring a freshly prepared sample to the solution of the salt of easily reducible metal and then use of cathodic polarization. This causes color effect as a result of optical phenomena like absorption and scattering of light by the deposited metal particles inside the pores. In this way, the oxide layer which was initially colorless can be converted to durably colored; usually there are shades of brown or black.

Electrochemical technologies of coloring anodized aluminum were developed in the 1970s and it is associated with the names of researchers such as Caboni, Langbein, Pfanhauser, Assad, and Sheasby [49]. Herrmann [50] gives 93 examples of electrochemical coloring processes using solutions of salts of the following metals: Pb, Cd, Cr, Fe, Au, Co, Cu, Mn, Ni, Se, Ag, Te, Zn, Sn. If an additional modification of the shape of the pores is introduced before the metal deposition process, it is possible to get a new color effect due to the interference effect [51].

Electrochemical coloring method of anodized aluminum is currently widely used as durable, decorative surface treatment for aluminum components, particularly for construction and architecture applications. Usually, tin nanoparticles are deposited in the pores of AAO using alternating AC or pulse current. When only cathodic polarization is implemented in that process, there is a risk of damage to the oxide layer.

The mechanism of electrodeposition of metals in the pores of the oxide layer was investigated by Skominas et al. [52] and Zemanova et al. [53] and lately by Bograchev et al. [54]. The effects of the reduction reaction of hydrogen ions and of the current frequency were studied.

Wider research in this field was provided by Tomassi [55].

Anodic oxidation of 99.5% Al samples was conducted in 1.75 M H_2SO_4 solution in temperature 20°C with voltage 16 V. Thickness of oxide layer obtained was 15 μm. The oxide layers from phosphoric acid solutions were also obtained. The electrodeposition of nickel, copper, tin, or silver was performed in temperature 25°C in the following solutions:

a) $NiSO_4$ 0,1 M	b) $CuSO_4$ 0,1 M	c) $SnSO_4$ 0,1 M	d) $AgNO_3$ 0.01 M
H_3BO_3 0,5 M	H_2SO_4 0,05 M	H_2SO_4 0,2 M	H_2SO_4 0,1 M

The maximum voltage of alternating current was 16 V (Ni) or 14 V (Cu, Sn, Ag). Usually, the frequency 50 Hz was used, but wide range from 0.1 to 1000 Hz was checked.

Electrochemical investigations have been performed using transient curves method, polarization methods, and impedance spectroscopy.

The uniform composite layers were obtained in the frequency region 10 – 100 Hz. With frequencies below 10 Hz the defects in oxide layer appear. In the high frequency region under 500 Hz the electrodeposition does not occur and high capacity current is observed.

Chemical analyses of obtained composite layers as well as structure, magnetic, microbiological properties, gravimetric and electrochemical investigations have been performed.

The X-ray analysis has confirmed that the metal deposition starts at the bottom of the pores close to the aluminum surface and the volume occupied by metal increases.

The investigations performed by transmission microscopy have shown that all pores are filled by metal deposit (Figure 4). The diameter of metal particles depends on pore diameter and has been found to be from 5 to 30 nm.

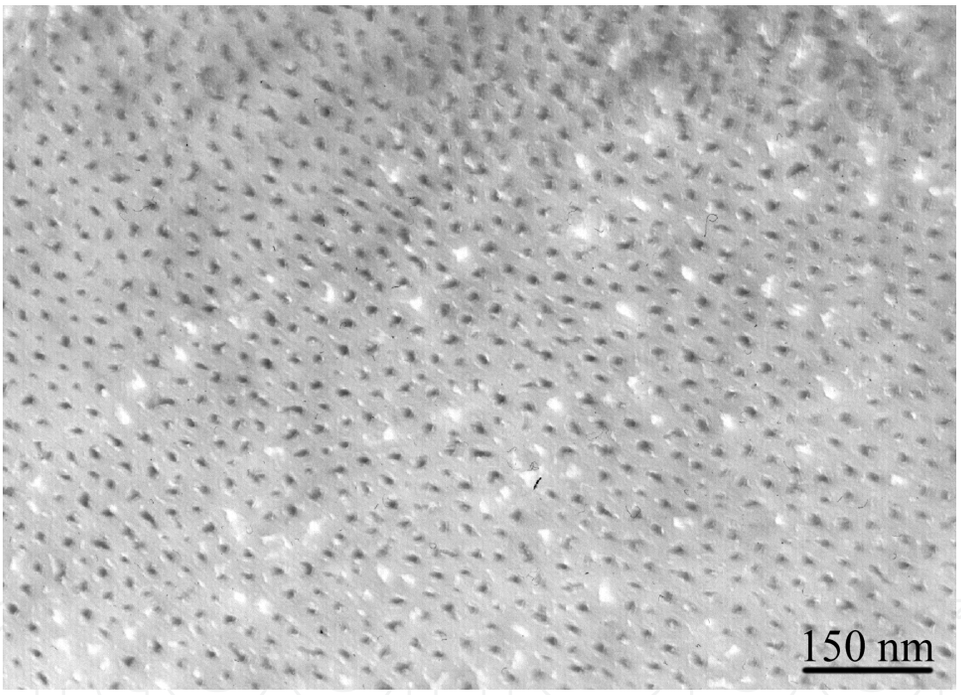

Figure 4. TEM image of AAO obtained in 1.75 M sulfuric acid, 20^{O}C, 16 V, 30 min with nickel nanoparticles, AC nickel deposition, 2 min.

The role of alternating polarization in metal deposition process can be clarified as a result of the investigations. In the cathodic cycles, the hydrogen ions' reduction occurs simultaneously to metal electrodeposition. The diffusion of hydrogen ions inside the oxide layer leads to formation of hydrogen bonds and hydrated regions of higher conductivity (active sites) are created. In these regions, the probability of electron transport is higher than in the other sites, where the current is mainly of ionic character. In the cathodic cycles, the new active sites are formed and filled by metal deposit.

http://dx.doi.org/10.5772/61263

In the anodic cycles, the repassivation of active sites occurs. This process ensures that the barrier layer is not damaged. The metal electrodeposition can then be effectively conducted with the formation of a uniform oxide–metal composite coating.

The optimum current frequencies are in good correlation with a time of charge carriers formation determined for aluminum oxide layers by Ebling [56], Hassel, and others [57-58]. Authors of this chapter have obtained composite layers consisting of the following metals: Ni, Cu, Sn, Fe, Co, Zn, Cd, Au, Pd, Ag.

Metal nanoparticles deposited with the method described above may create durable system with an oxide matrix characterized with interesting scientific and operation properties. Metal nanoparticles can also be separated from the matrix, after, for example, a selective dissolution of alumina, and then examined individually. Nanowires, nanotubes, or nanodots can be similarly obtained. The TEM image of AAO layer with nickel nanoparticles is shown in Figure 4. The bigger diameter of metal nanostructures can be obtained when the oxide matrix is formed in phosphoric acid solution. The AAO formed in phosphoric acid is presented alone in Figure 5 and with nickel nanostructures in Figures 6 and 7.

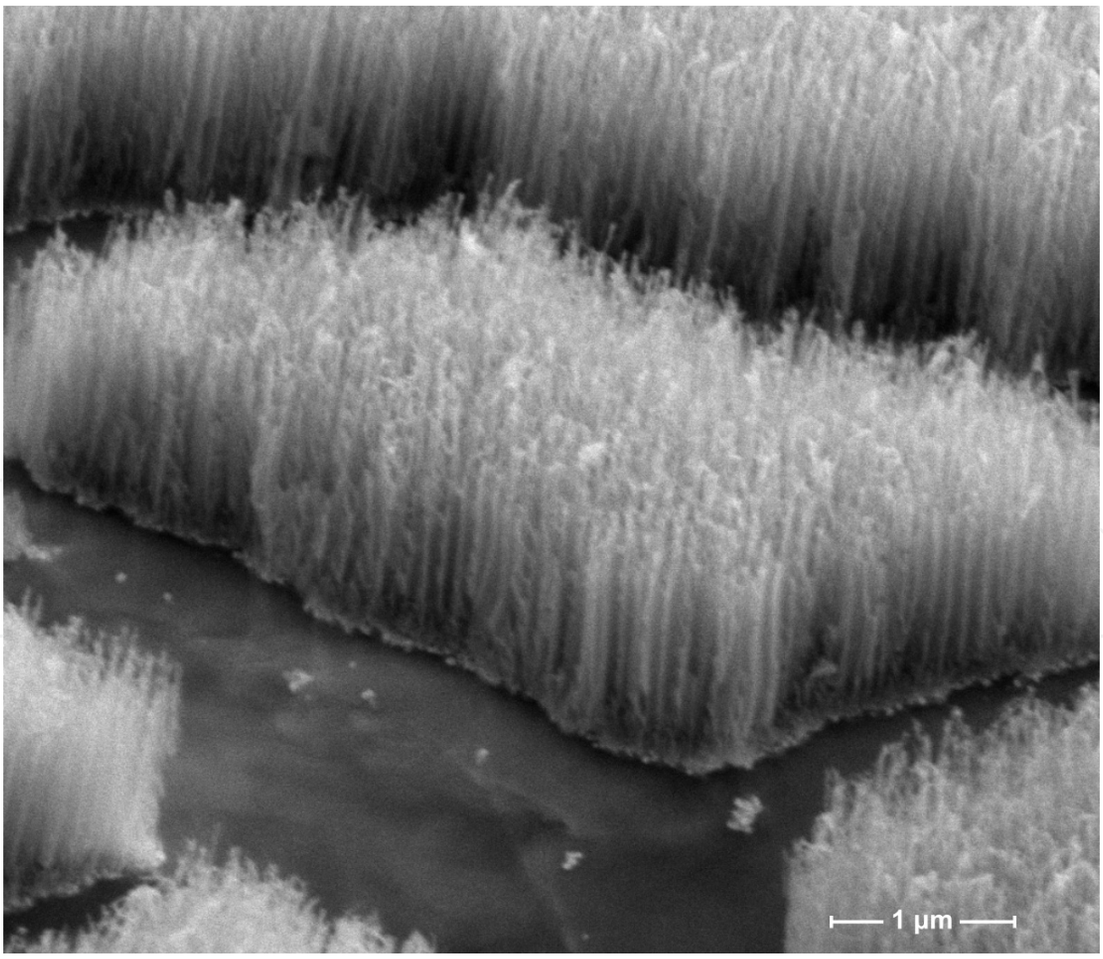

Figure 5. SEM image of AAO obtained in 500 g/dm^2 phosphoric acid, 30^{O}C, 30 V, 20 min.

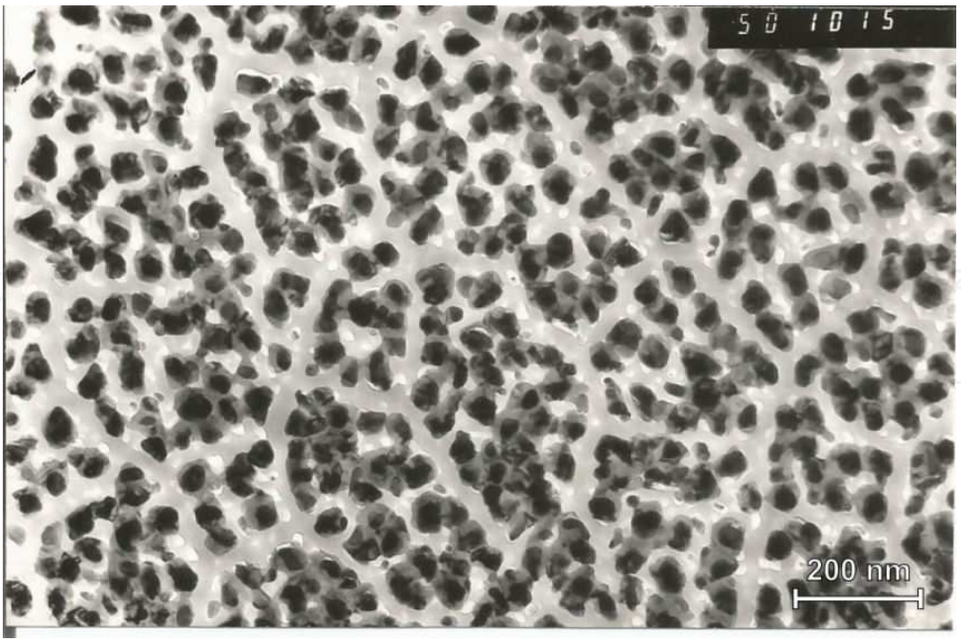

Figure 6. SEM image of AAO obtained in phosphoric acid with nickel particles. AC nickel deposition, 30 V, 30 s.

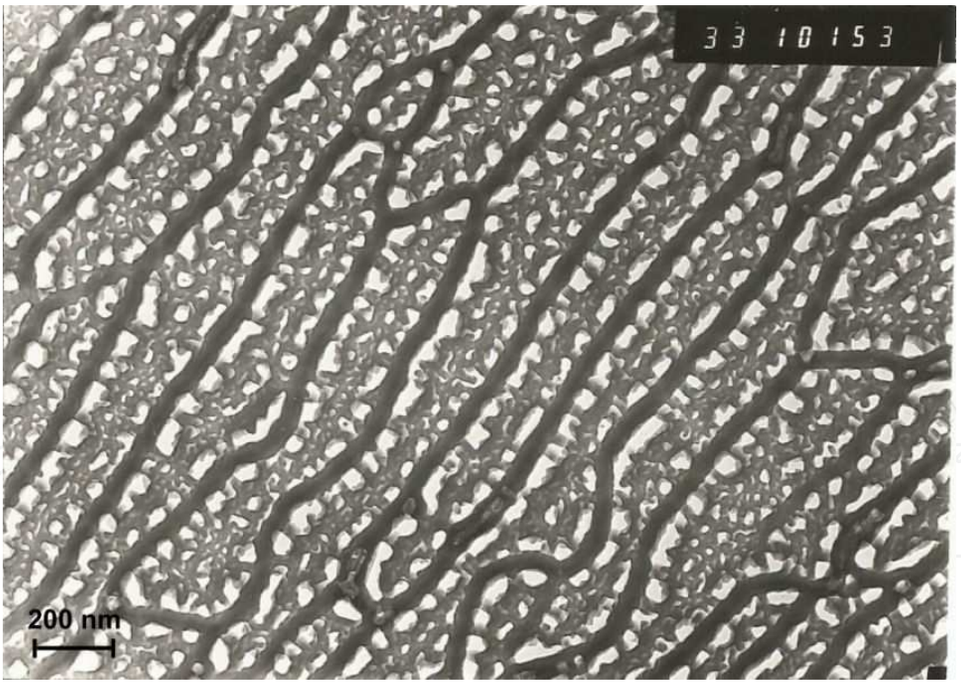

Figure 7. SEM image of AAO obtained in phosphoric acid with nickel particles. AC nickel deposition, 40 V, 15 s.

Oxide layers can be of different porosity with branches when anodic oxidation process is unsteady. The pore branching is clearly visible in the SEM photograph of the oxide layer obtained in a solution of sulfosalicylic acid (Figure 8). After deposition of the metal within the pores of oxide layer, the structure of metal nanoparticles is complex, e.g., in the form of

http://dx.doi.org/10.5772/61263

branches [59-60] as is shown in Figure 9. Anodic oxidation was performed in oxalic acid solution; various barrier layer thinning procedures (BLT) were used before metal deposition. Metal structures deposited with DC are usually compact, but when AC pulse current is implemented, they may be of grained structure.

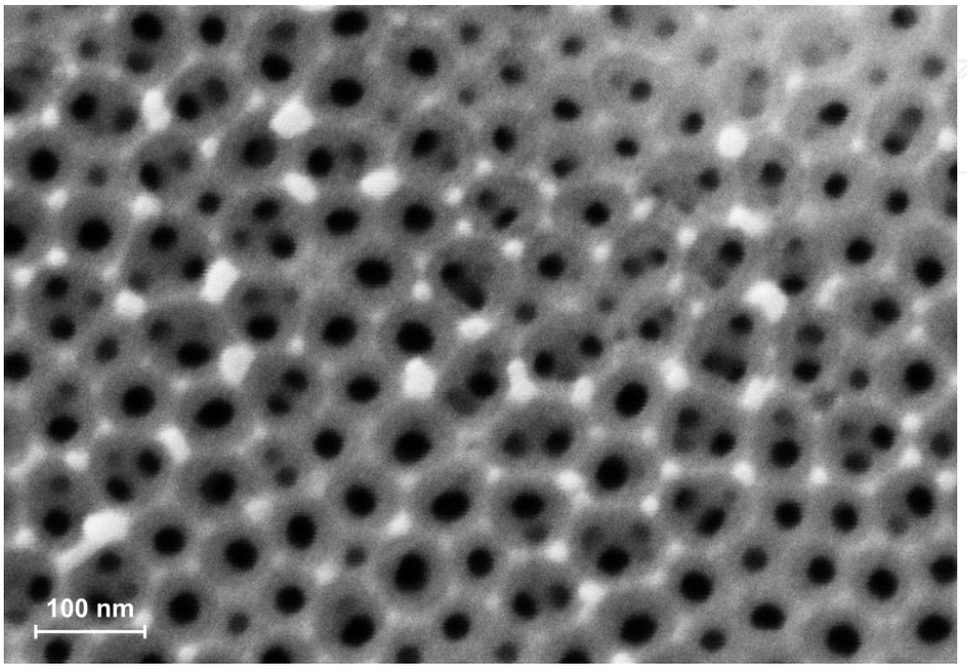

Figure 8. SEM image of AAO coating obtained in solution of sulfosalicylic acid 50 g/dm^3, oxalic acid 10 g/dm^3 and sulfuric acid 5 g/dm^3, 3 A/dm^2, 20^{O}C, 30 min [114].

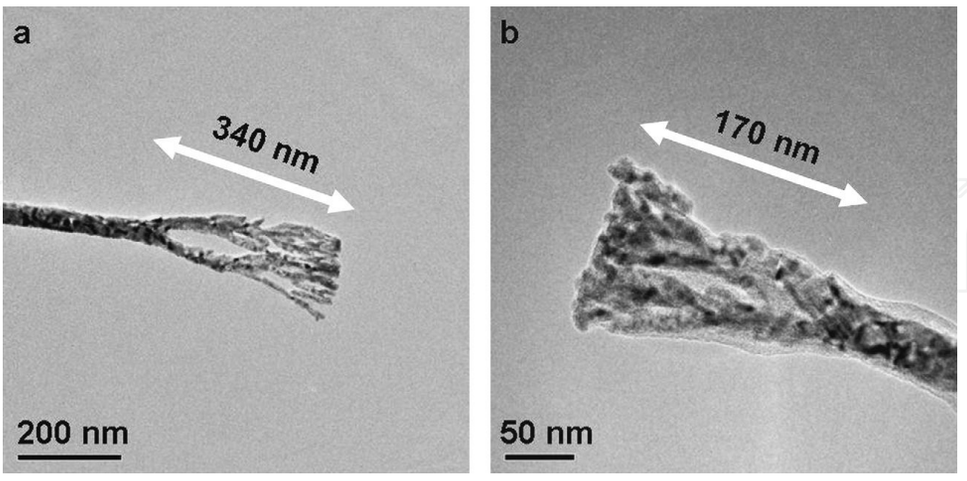

Figure 9. Nickel branches obtained by anodic oxidation in oxalic acid, 20^{O}C, 45 V, 1 h, and nickel pulse electrodeposition from Watt's solution with various BLT procedures (Permission Elsevier [59]).

In the processes for preparing metallic nanostructures with the use of AAO layers, sometimes additional operations are applied in order to obtain geometrically complex systems, e.g., PVD

methods, photochemical techniques, and other methods. An excellent overview of these methods can be found in the monograph of Jani et al. [61]. Some examples of complex manufacturing of anodic oxide layer and forming of the metal nanostructures are given in Table 5.

No.	Process	References
1.	Evaporation of aluminum 0.3–1 μm layer on oxide surface. After using a lithographic process the regular patterns of porous oxide were obtained.	[62]
2.	Micropatterned substrates were prepared by fabrication of polyethylene glycol hydrogel microstructures on alumina membranes with 200 nm nanopores using photolitography.	[63]
3.	Electroless deposition of nickel–boron nanoparticle structures on AAO membrane.	[64]
4.	AAO membranes were immersed in $AgNO_3$ solution. As a result of hydrothermal reaction, the Ag nanoflakes were obtained on the oxide membrane surface.	[65]
5.	The AAO membranes were fabricated by a two-step anodizing of AA 1050 alloy followed by removal of Al and pore opening/widening procedure. Au conducting layer was sputtered on one side of AAO membrane. The dense arrays of Ag, Au, and Sn nanowires were fabricated by a DC electrochemical deposition process.	[66]
6.	Thin Au films with highly ordered arrays of hemispherical dots were fabricated by evaporating Au on the surface of porous anodic alumina template.	[67]
7.	Highly ordered arrays of Ni nanoholes and FeNi dots were prepared by sputtering and replica processing techniques using nanoporous alumina membranes as a template.	[68]

Table 5. Examples of complex methods of preparation of oxide templates and metal nanostructures

5. Emerging applications

Electrochemically obtained porous layers of aluminum oxide are widely used in nanotechnology, not only in scientific research but also in various applications. Porous oxide layer can be separated from the substrate. After removing the barrier layer membranes are obtained. They can be applied for example in nanofiltration for removing bacteria from medical preparations (cold sterilization). They are also used to prepare the solutions of test samples for liquid chromatography. Revised filtration properties of these membranes can be found in Lee et al. [69].

http://dx.doi.org/10.5772/61263

Alumina is insoluble, nontoxic, and characterizes excellent biocompatibility. AAO porous layer has a highly developed surface area – about 2 to 3 orders of magnitude higher than the surface of the aluminum substrate. Hence, importance of these materials is growing and they are more widely used in chemical catalysis, in bioreactors, and in sensors. Porous anodic alumina is also an excellent substrate for culturing bacteria in discrete growth compartments. These cultures are investigated with the use of fluorescence microscopy. A broad overview of the use of the porous AAO in biotechnology is presented by Ingham et al. [70]. They present the list of fields of AAO applications as follows:

- Counting and cell identification
- Growth and microcolony imagimg of microorganisms on AAO
- High-throughput microbiology
- Physical detection technologies

The unique properties of porous AAO are used in sensors and biosensors as already mentioned. A review article was published by Santos et al. [71] in which authors distinguished two types of AAO sensors: optical and electrochemical. The phenomena and techniques used in both types of sensors are summarized as follows:

Optical Biosensors

- Photoluminescence (PL) spectroscopy
- Surface-plasmon resonance (SPR)
- Waveguiding spectroscopy (WS)
- Localized surface-plasmon resonance (LSPR)
- Surface-enhanced Raman scattering spectroscopy (SERS)
- Reflectometric interference spectroscopy (RIfS)

Electrochemical Sensors and Biosensors

- Voltammetric and amperometric
- Impedance spectroscopy (IS)
- Capacitive, conductometric, and resistive sensors

Sensors and biosensors with AAO are used for the detection of gases, vapors, organic molecules, biomolecules, DNA, proteins, antibodies and cells, viruses, bacteria, cancer cells, which are in air, water, and biological environments.

As described in the previous chapter, complex composite systems produced by deposition inside the pores of AAO additional phases of metal, carbon, inorganic or organic compounds have been widely used in basic research and applications. This is especially due to their unique features like electrical, optical, catalytic, biological, and other properties. Major applications and references to the literature are given in Table 6.

No.	Application	Foreign phases in AAO matrix	References
1.	Membranes for ultra- and nanofiltration		[69,73]
2.	Sensors and biosensors		[71,72]
3.	Decorative coatings on aluminum	Sn, Ni, Cu	[20]
4.	Formation of metal nanoparticles and nanowires	Fe, Ni, Co, Au, Ag, Cu, Bi, Pt, Pd, Sn, W, Zn, Sb, Se, alloys	[66,74,75]
5.	Formation of dots and nanodots	InAs, SiGe, Si, CdTe, GaAs, Fe, Ag	[67,68,76,77]
6.	Formation of carbon structures, carbon nanotubes, graphene	C	[78-84]
7	Formation of inorganic compounds nanoparticles	GaN, ZnO, CdS, AgI, PbS	[85,86]
8.	Formation of organic compounds nanoparticles	Polypyrrole, polyaniline, DNA, polythiophene, ethylene vinyl acetate copolymer	[87,88]
9.	Examination of optical systems and models	Ni, Co	[64,89,90]
10.	Examination of magnetic systems and models	Fe, Ni, Co, alloys	[91-93]
11.	Catalysts of chemical reactions	Ni, Au, Pd, C	[81,94,95]
12.	Electronic components, capacitors, semiconductors	C, CdS, ZnO, compounds of In, Ga	[80,96-98]
13.	Luminescence, electroluminescence, and photoluminescence devices	Cu_2O, ZnS, In_2O_3	[96,99-102]
14.	Magnetic systems, data storage	Fe, Ni, Co, alloys Pt	[103-105]
15.	Sliding joints	MoS_2, Sn	[106]
16.	Solar collectors	Ni, Sn	[20]
17.	Solar batteries	CdS	[107,108]
18.	Lithium-ion batteries	$LiMn_2O_4$, CdS, CoSb	[109]
19.	Antibacterial materials	Ag	[110]
20.	Photonic crystals		[111,112]
21.	Fuel cells	Solid acid	[113]

Table 6. Main applications of AAO layers in science, technology, and nanotechnology

http://dx.doi.org/10.5772/61263

6. Summary

The structure of AAO layers can be precisely controlled with operation parameters of electrochemical oxidation. Complicated and expensive apparatus is not required for their preparation. It is for this reason that these layers are so widely used in nanotechnology.

Using a variety of techniques, in particular electrochemical methods, various composite materials of alumina and the foreign phase can be prepared with new or improved physical or chemical properties. AAO template having a uniform porous structure allows obtaining sustainable systems of nanoparticles, nanowires, nanotubes, and nanodots with an unlimited number of materials. AAO has become in recent years one of the most important materials for nanotechnology development, both in research as well as in applications.

The significant number of publications in this field now exceeds the size of one hundred items per year. Further applications of the AAO as nanofiltration membranes are anticipated, including drug delivery, gas permeation, and hemodialysis. Flat membranes are already commercially available and now efforts have been made to prepare tubular membranes [69].

In biomedical applications, AAO has been confirmed as a good substrate for the study of biomolecules, cells, and bacteria and their detection by means of optical imaging methods (SERS, optical waveguides), and fluorescence-based detection methods [70].

In the field of sensors and biosensors, AAO applications allow to broaden choice and miniaturization of sensors, especially those with optical measurements. The design of implantable biosensors with the ability to monitor biological systems in vivo and real time is promising for the application of AAO immunosensors [71-72].

It seems that in order to further the development of manufacturing methods and applications of metal nanostructures, it is advisable to develop further research in the following areas:

1. Basic research on the process of electrochemical oxidation of aluminum and of forming a specific porous structure of oxide layers.
2. Improving the methods of producing the best quality AAO with regular distribution of pores and desired pores geometry.
3. Further study of the effects of various factors on the structure and chemical composition of the AAO, such as:
    - Multistage oxidation
    - Use programmable waveform pulse currents
    - The importance of the pretreatment of the surface of aluminum substrate (alloy type, its structure, impurities)
    - Effect of heat pretreatment of the substrate and the final thermal treatment of AAO layer
4. Basic research of electrodeposition of metals in the pores of oxide layers.

5. The use of nonaqueous solutions or mixed solvents for metal deposition. In this way, the range of materials (metals and alloys) for nanostructures creations can be extended.

6. Study of the effect of complex current characteristics, including pulse current on electrodeposition processes of metals in the AAO template.

7. Examination of the physical (electrical, optical, magnetic, etc.) and chemical properties (catalytic, antibacterial, etc.); research on novel systems of metal nanoparticles and their alloys in a matrix of alumina or separated from oxide matrix.

Author details

Piotr Tomassi* and Zofia Buczko

*Address all correspondence to: piotr.tomassi@gmail.com

Institute of Precision Mechanics, Warsaw, Poland

References

[1] Romanowski W. *Highly Dispersed Metals*. Warszawa: PWN - Polish Scientific Publishers; 1987, Chichester: Ellis Horwood Limited Publishers; 1987, pp. 61-87.

[2] Feldheim DL, Colby AF.Jr. *Metal Nanoparticles. Synthesis, Characterization and Applications*. New York: Marcel Dekker, Inc.; 2002, pp. 119-139.

[3] Lin Q, Sun Zh. Study on optical properties of aggregated ultra-small metal nanoparticles. *Optik* 2011;122 1031-1036.

[4] Noguez C. Optical properties of isolated and supported metal nanoparticles. *Optic Mater* 2005;27 1204-1211.

[5] Wu B, Yuan H, Kuang A, Chen H, Zhang S. Static electric and optical properties of two coupled noble metal nanoparticles. *Comput Mater Sci* 2012;51 430-436.

[6] Kim JH, Yoon ChS. Modification of magnetic properties of metal nanoparticles using nanotemplate approach. *Thin Solid Films* 2008;516 4845-4850.

[7] Keller F, Hunter MS, Robinson DL. Structural features of oxide coatings on aluminium. *J Electrochem Soc* 1953;100(9) 411-419.

[8] Murphy JF, Michelson CE. A theory for the formation of anodic oxide coatings on aluminium. Proceedings of the Conference on Anodizing Aluminium, 1961, Nottingham UK, p. 83-95.

[9] Palibroda E, Lupsan A, Pruneanu S, Saros M. Aluminium porous oxide growth. On the electric conductivity of the barrier layer. *Thin Solid Films* 1995;256(1-2) 101-105.

[10] Palibroda E. Aluminium porous oxide growth. II On the rate determining step. *Electrochim Acta* 1995;40(8) 1051-1055.

[11] Brace AW. *The technology of anodizing aluminium*, Interall S.r.l. Publishers, Modena, 2000, Italy, pp. 1-12.

[12] Wielage B, Alisch G, Lampke Th, Nickel D. Anodizing – a key for surface treatment of aluminium. *Key Engin Mater* 2008;384, 263-281.

[13] Parkhutik VP, Shershulsky VI. Theoretical modelling of porous oxide growth on aluminium. *J Physics D: Physics* 1992;25 1258-1263.

[14] Kanakala R, Singaraju PV, Venkat R, Das B. Modeling of porous alumina template formation under constant current conditions. *J Electrochem Soc*, 2005;152(1) 31-35.

[15] Singaraju P, Venkat R, Kanakala R, Das B. Model for porous alumina formation. Constant voltage anodization. *Euro Physic J, Appl Physics* 2006;35 107-111.

[16] Houser JE, Hebert HR. Modeling the potential distribution in porous anodic alumina films during steady-state growth. *J Electrochem Soc* 2006; 153(12) B566-B573.

[17] Wu Z, Richter C, Menon L, A study of anodization process during pore formation in nanoporous alumina templates. *J Electrochem Soc* 2007;154(1), E8-E12.

[18] Cheng Ch, Ngan AHW. Modelling and simulation of self-ordering in anodic porous alumina. *Electrochim Acta* 2011;56 9998-10008.

[19] Tomassi P. Mathematical model of anodic oxidation of aluminium. In: *Surface Treatment of Aluminium and other Light Metals*. Saulgau: Eugen G. Leuze Verlag; 1993. p. 14-18.

[20] Wernick S, Pinner R, Sheasby PG. *The Surface Treatment and Finishing of Aluminum and its Alloys*. Teddington: Finishing Publications Ltd.; 1987, pp. 289-368.

[21] Li XF. Chen D. Chen Zh. Wu Y, Wang ML, Ma N, Wang H. Stability of nanopore formation in aluminum anodization in oxalic acid. *Transact Nonferrous Mater Soc China* 2012;22 105-109.

[22] Han XY, Shen WZ. Improved two-step anodization technique for ordered porous anodic aluminum membranes. *J Electroanalytic Chem* 2011;655 56-64.

[23] Araoyinbo AO, Fauzi MNA, Sreekantan S, Aziz A. A novel process to produce nanoporous aluminum oxide using titration technique. *J Non-Crystalline Solids* 2010;356 1057-1060.

[24] Ono S, Saito M, Asoh H. Self-ordering of anodic porous alumina formed in organic acid electrolytes. *Electrochim Acta* 2005;51 827-833.

[25] Jia Y, Zhou H, Luo P, Chen J, Kuang Y. Preparation and characteristics of well-aligned macroporous films on aluminum by high voltage anodization. *Surf Coat Technol* 2006;201 513-518.

[26] Qin X, Zhang J, Meng X, Deng Ch, Zhang L, Ding G, Zeng H, Xu X. Preparation and analysis of anodic aluminum oxide films with continuously tunable interpore distances. *Applied Surface Science* 2015;328 459-465.

[27] Mozalev A, Mozaleva I, Sakairi M, Takahashi H. Anodic film growth on Al layers and Ta-Al metal bilayers in citric acid electrolytes. *Electrochimica Acta* 2005;50 5065-5075.

[28] Schwirn K, Lee W, Hillebrand R, Steinhart M, Nielsch K, Gosele U. Self-ordered anodic aluminum oxide formed by H_2SO_4 hard anodization. *ACS Nano* 2008;2(2) 302-310.

[29] Zaraska L, Sulka GD, Jaskuła M. Porous anodic alumina membranes formed by anodization of AA1050 alloy as templates for fabrication of metallic nanowire arrays. *Surf Coat Technol* 2010;205 2432-2437.

[30] Kirchner A, MacKenzie KJD, Brown IWN, Kemmitt T, Bowden ME. Structural characterisation of heat-treated anodic alumina membranes prepared using a simplified fabrication process. *J Membrane Sci* 2007;287 264-270.

[31] Bocchetta P, Sunseri C, Chiavarotti G, Di Quarto F. Microporous alumina membranes electrochemically grown. *Electrochim Acta* 2003;48 3175-3183.

[32] Zhao X, Seo SK, Lee UJ, Lee KH. Controlled electrochemical dissolution of anodic aluminum oxide for preparation of open-through pore structures. *J Electrochem Soc* 2007;154(10) C553-C557.

[33] Ginder RS, Hersam MC, Lipson AL. Unique pore-formation geometries in anodized aluminum oxide. *Nanoscope* 2010;7(1) 48-51.

[34] Nguyen TN, Kim D, Jeong DY, Kim MW, Kim JU. Formation behavior of nanoporous anodic aluminum oxide film in hot glycerol/phosphate electrolyte. *Electrochim Acta* 2012;83 288-293.

[35] Michalska-Domańska M, Norek M, Stępniowski WJ, Budner B. Fabrication of high quality anodic aluminum oxide (AAO) on low purity aluminum – a comparative study with the AAO produced on high purity aluminum. *Electrochim Acta* 2013;105 424-432.

[36] Li Y, Zheng M, Ma L, Shen W. Fabrication of highly ordered nanoporous alumina films by stable high-field anodization. *Nanotechnology* 2006;17 5101-5105.

[37] Lee W, Schwirn K, Steinhart M, Pippel E, Scholz R, Gosele U. Structural engineering of nanoporous anodic aluminum oxide by pulse anodization of aluminum. *Nanotechnology* 2008;3 234-239.

[38] Chung CK, Liao MW, Lee CT. Effects of temperature and voltage mode on nanoporous anodic aluminum oxide films by one-step anodization. *Thin Solid Films* 2011;520 1554-1558.

[39] Chung CK, Chang WT, Liao MW, Chang HC, Lee CT. Fabrication of enhanced anodic alumina oxide performance at room temperature using hybrid pulse anodization with effective cooling. *Electrochim Acta* 2011;56 6489-6497.

[40] Pashchanka M, Schneider JJ. Umiform contraction of high-aspect-ratio nanochannels in hexagonally patterned anodic alumina films by pulsed voltage oxidation. *Electrochim Acta* 2013;34 263-265.

[41] Su SH, Li CH, Zhang FB, Yokoyama M. Characterization of anodic aluminium oxide pores fabricated on aluminium templates. *Superlattices Microstruct* 2008;44 514-519.

[42] Sulka GD, Stępniowski WJ. Structural features of self-organized nanopore arrays formed by anodization of aluminum in oxalic acid at relatively high temperatures. *Electrochim Acta* 2009;54 3683-3691.

[43] Cui J, Wu Y, Wang Y, Zheng H, Xu G, Zhang X. A facile and efficient approach for pore-opening detection of anodic aluminum oxide membranes. *Appl Surf Sci* 2012;258 5305-5311.

[44] Zaraska L, Stępniowski WJ, Ciepiela E, Sulka GD. The effect of anodizing temperature on structural features and hexagonal arrangements of nanopores in alumina synthesized by two-step anodizing in oxalic acid. *Thin Solid Films* 2013;534 155-161.

[45] Zaraska L, Stępniowski WJ, Jaskuła M, Sulka GD. Analysis of nanopore arrangement of porous alumina layers formed by anodizing in oxalic acid at relatively high temperatures. *Appl Surf Sci* 2014;305 650-657.

[46] Asoh H, Ono S, Hirose T, Nakao M, Masuda H. Growth of anodic porous alumina with square cells. *Electrochim Acta* 2003;48 3171-3174.

[47] Choi J, Wehrspohn RB, Gosele U. Mechanism of guided self-organization producing quasi-monodomain porous alumina. *Electrochim Acta* 2005;50 2591-2595.

[48] Randon J, Mardilovich PP, Govyadinov AN, Paterson R. Computer simulation of inorganic membrane morphology Part 3. Anodic alumina films and membranes. *J Colloid Interf Sci* 1995;169 335-341.

[49] Sheasby PG, Cooke WE. The electrolytic colouring of anodized aluminium. *Transact Inst Metal Finish* 1974;52(3) 103-106.

[50] Herrmann E. Elektrolytisches Farben von anodisiertem Aluminium. *Galvanotechnik* 1972;63(2) 110-121.

[51] Sheasby PG, Patrie J, Badia M, Cheetham G. The colouring of anodized aluminium by means of optical interference effects. *Transact Inst Metal Finish* 1980;58(2) 41-47.

[52] Skominas V, Lichusina S, Miecinskas P, Jagminas A. A voltammetric and chronopotentiometric study of anodized aluminium in metal salt solutions. *Transact Inst Metal Finish* 2001;79(6) 213-218.

[53] Zemanova M, Gal M, Chovanceva M. Effect of frequency on pulse electrolytic colouring process of anodised aluminum. *Transact Inst Metal Finish* 2009;87(2) 97-101.

[54] Bograchev DA, Volgin VM, Davydov AD. Simple model of mass transfer in template synthesis of metal ordered nanowire. *Electrochimica Acta* 2013;96 1-7.

[55] Tomassi P. Electrochemical reactions to form composite layers aluminium oxide – metal. *Acta Physica Polonica A* 2002;102(2) 215-220.

[56] Ebling D. *Elektronische und Ionische Prozesse in Submikronstrukturen und deren Praparation im System Al/Al_2O_3*. PhD Thesis. Heinrich Heine University Dusseldorf; 1991. pp. 52-102.

[57] Hassel AW, Lohrengel MM. Initial stages of cathodic breakdown of thin anodic aluminium oxide films. *Electrochim Acta* 1995;40(4) 433-437.

[58] Hassel AW, Lohrengel MM, Schulze JW. Ultradunne Aluminiumoxid-Schichten. Untersuchung elektronischer und ionischer Transportprozesse. *Matalloberflache* 1996;50(1) 19-22.

[59] Montenero-Moreno JM, Belenguer M, Sarret M, Muller CM. Production of alumina templates suitable for electrodeposition of nanostructures using stepped techniques. *Electrochim Acta* 2009;54 2529-2535.

[60] Cheng W, Steinhart M, Gosele U, Wehrspon RB. Tree-like alumina nanopores generated in non-steady-state anodization. *J Mater Chem* 2007;17 3493-3495.

[61] Jani AMM, Losic D, Voelcker NH. Nanoporous anodic aluminium oxide: Advances in surface engineering and emerging applications. *Progress Mater Sci* 2013;58 636-704.

[62] Li AP, Muller F, Birner A, Nielsch K, Gosele U. Fabrication and microstructuring of hexagonally ordered two-dimensional nanopore arrays in anodic alumina. *Adv Mater* 1999;11(6) 483-487.

[63] Lee HJ, Kim DM, Park S, Lee Y, Koh WG. Micropatterning of a nanoporous alumina membrane with poly(ethylene glycol) hydrogel to create cellular micropatterns on nanotopographic substrates. *Acta Biomaterialia* 2011;7 1281-1289.

[64] Durtschi JD, Erali M, Herrmann MG, Elgort MG, Voelkerding KV, Smith RE. Optically improved aluminum oxide membrane through electroless Ni modification. *J Membrane Sci* 2005;248 81-87.

[65] Li X, Dong K, Tang L, Wu Y, Yang P, Zhang P. The fabrication of Ag nanoflake arrays via self-assembly on the surface of an anodic aluminum oxide template. *Appl Surf Sci* 2010;256 2856-2858.

[66] Zaraska L, Sulka GD, Jaskuła M. Porous anodic alumina membranes formed by anodization of AA1050 alloy as templates for fabrication of metallic nanowire arrays. *Surf Coat Technol* 2010;205 2432-2437.

[67] Gao T, Fan JC, Meng GW, Chu ZQ, Zhang LD. Thin Au film with highly ordered arrays of hemispheral dots. *Thin Solid Films* 2001;401 102-105.

[68] Vazquez M, Pirota KR, Navas D, Asenjo A, Hernandez-Velez M, Prieto P, Sanz JM. Ordered magnetic nanohole and antidot arrays prepared through replication from anodic alumina templates. *J Magnet Magnetic Mater* 2008;320 1978-1983.

[69] Lee KP, Mattia D. Monolithic nanoporous alumina membranes for ultrafiltration applications: Characterization, selectivity-permeability analysis and fouling studies. *J Membrane Sci* 2013;435 52-61.

[70] Ingham CJ, ter Maat J, de Vos WM. Where bio meets nano: The many uses for nanoporous aluminum oxide in biotechnology. *Biotechnol Adv* 2012;30 1089-1099.

[71] Santos A, Kumeria T, Losic D. Nanoporous anodic aluminum oxide for chemical sensing and biosensors. *Trends Analytic Chem* 2013;44 25-38.

[72] Koh G, Agarwal S, Cheow P.S, Tob CS. Development of membrane-based electrochemical immunosensor. *Electrochim Acta* 2007;53 803-810.

[73] Tomassi P, Buczko Z. Ultrafiltration membranes obtained by anodic oxidation of aluminium. *Proceedings of the V International Symposium "Forum Chemiczne '99'"*, Warszawa, 19-21 April, 1999. p. 181.

[74] Evans P, Hendren WR, Atkinson R, Wurtz GA, Dickson W, Zayats AV, Pollard RJ. Growth and properties of gold and nickel nanorods in thin film alumina. *Nanotechnology* 2006;17 5746-5753.

[75] Feliciano J, Martinez-Ifiesta MM. Synthesis and characterization of Pd, Cu and Ag nanowires in anodic alumina membranes using solid state reduction. *Mater Lett* 2012;82 211-213.

[76] Liang J., Luo H., Beresford R., Xu J. A growth pathway for highly ordered quantum dot arrays. *Appl Physics Lett* 2004;85 5974-5976.

[77] Jung M, Lee HS, Park HL, Mho S. Fabrication of high density CdTe/GaAs nanodot arrays using nanoporous alumina masks. *Curr Appl Physics* 2006;6S1 e187-e191.

[78] Ciambelli P, Arurault L, Sarno M, Fontorbes S, Leone C, Datas L, Sannino D, Lenormand P, Le Blond Du Plony S. Controlled growth of CNT in mesoporous AAO through optimized conditions for membrane preparation and CVD. *Nanotechnology* 2011;22(265613) 1-12.

[79] Jang WY, Kulkarni NN, Shih CK., Yao Zh. Electrical characterization of individual carbon nanotubes grown in nanoporous anodic alumina templates. *Appl Physics Lett* 2004;84(7) 1177-1179.

[80] Ahn HJ, Sohn JI, Lim YS, Shim HS, Kim WB, Seong TY. Electrochemical capacitors fabricated with carbon nanotubes grown within the pores of anodized aluminum oxide. *Electrochem Commun*. 2006;8(4) 513-516.

[81] Sigurdson S, Sundaramurthy V, Dalai AK, Adjaye J. Effect of anodic alumina pore diameter variation on template-initiated synthesis of carbon nanotube catalyst supports. *J Mol Cataly A: Chemical* 2009;306(1-2) 23-32.

[82] Jeong B, Uhm S, Kim JH, Lee J. Pyrolitic carbon infiltrated nanoporous alumina reducing contact resistance of aluminium/carbon interface. *Electrochim Acta* 2013;89(1) 173-179.

[83] Tu JP, Zhu LP, Hou K, Guo SY. Synthesis and frictional properties of array film of amorphous carbon nanofibres on anodic aluminium oxide. *Carbon* 2003;41(6) 1257-1263.

[84] Tu JP, Zhu LP, Hou K, Guo SY. Synthesis and frictional properties of array film of amorphous carbon nanofibres on anodic aluminium oxide. *Carbon* 2003;41(6) 125-1263.

[85] Cheng GS, Chen SH, Zhu XG, Mao YQ, Zhang LD. Highly ordered nanostructures of single crystalline GaN nanowires in anodic alumina membranes. *Mater Sci Engin* A 2000;286 165-168.

[86] Gomez H, Riveros G, Ramirez D, Henriquez R, Schrebler R, Marotti R, Dalchiele E. Growth and characterization of ZnO nanowire arrays electrodeposited into anodic alumina templates in DMSO solution. *Appl Physics A* 2012;16 197-204.

[87] Al-Kaysi RO, Bardeen CJ. General method for the synthesis of crystalline organic nanorods using porous alumina templates. *Chem Commun* 2006; 1224-1226.

[88] Cheng FL, Zhang ML, Wang H. Fabrication of polypyrrole nanowire and nanotube arrays. *Sensors* 2005;5 245-249.

[89] Li L. AC anodization of aluminum, electrodeposition of nickel and optical property examination. *Solar Energy Mater Solar Cells* 2000;64 279-289.

[90] Tang HJ, Wu FQ, Zhang S. Optical properties of Co/Al_2O_3 nano-array composite structure. *Appl Physics A* 2006;85 29-32.

[91] Metzger RM, Konovalov VV, Sun M, Xu T, Zangari G, Xu B, Benakli M, Doyle W.D. Magnetic nanowires in hexagonally ordered pores of alumina. *IEEE Transact Magnetics* 2000;36(1) 30-35.

[92] Qin DH, Lu M, Li H.L. Magnetic force microscopy of magnetic domain structure in highly ordered Co nanowire arrays. *Chem Physics Lett* 2001;350 51-56.

[93] Hamrakulov B, Kim IS, Lee MG, Park BH. Electrodeposited Ni, Fe, Co and Cu single and multilayer nanowire arrays on anodic aluminum oxide template. *Transact Nonferrous Metals Soc China* 2009 19 83-87.

[94] Yu Y, Kant K, Shapter JG, Addai-Mensah J, Losic D. Gold nanotube membranes have catalytic properties. *Microporous Mesoporous Mater* 2012;153 131-136.

[95] Pellin MJ, Stair PC, Xiong G, Elam JW, Birrell J, Curtiss L, George SM, Han CY, Iton L, Kung H, Kung M, Wang HH. Nesoporous catalytic membranes. Synthetic control of pore size and wall composition. *Cataly Lett* 2005;102 127-130.

[96] Lei Y, Chim WK. Highly ordered arrays of metal/semiconductor core-shell nanoparticles with tunable nanostructures and photoluminescence. *J Am Chem Soc* 2005;127 1487-1492.

[97] Mardare AI, Kaltenbrunner M, Sariciftci NS, Bauer S, Hassel AW. Ultra-thin anodic alumina capacitor films for plastic electronics. *Physica Status Solidi* A 2012;209 813-818.

[98] Wen S, Mho S, Yeo IH. Improved electrochemical capacitive characteristics of the carbon nanotubes grown on the alumina templates with high pore density. *J Power Sources* 2006;163 304-308.

[99] Li GH, Zhang Y, Wu YC, Zhang LD. Photoluminescence of anodic alumina membranes: pore size dependence. *Appl Physics A* 2005;81 627-629.

[100] Chen JH, Huang CP, Chao CG, Chen TM. The investigation of photoluminescence centres in porous alumina membranes. *App Physics A* 2006;84 297-300.

[101] Ko E, Choi J, Okamoto K, Tak Y, Lee J. Cu_2O nanowires in an alumina template: Electrochemical conditions for the synthesis and photoluminescence characteristics. *Chem Phys Chem* 2006;7 1505-1509.

[102] Li GH, Zhang Y, Wu YC, Zhang LD. Photoluminescence of anodic alumina membranes: pore size dependence. *Appl Physics A* 2005;81 627-629.

[103] Chu Sz, Inoue S, Wada K, Kurashima K. Fabrication of integrated arrays of ultrahigh density magnetic nanowires on glass by anodization and electrodeposition. *Electrochim Acta* 2005;51 820-826.

[104] Yasui K, Morikawa T, Nishio K, Masuda H. Patterned magnetic recording media using anodic porous alumina with single domain hole confoguration of 63 nm hole interval. *Jap J Appl Physics* 2005;44 L469-L471.

[105] Seo BI, Shaislamov UA, Lee SJ, Kim SW, Kim IS, Hong SH, Yang B. Growth of ferroelectric BLT and Pt nanotubes for semiconductor memories. *J Crystal Growth* 2006;292 315-319.

[106] Yu D, Feng Y, Zhu Y, Zhang X, Li B, Liu H.Template synthesis and characterization of molybdenum disulfide nanotubes. *Mater Res Bull* 2011;46 1504-1509.

[107] Aguilera A, Jayaraman V, Sanagapalli S, Suresh Singh R, Jayaraman V, Sampson K., Singh V.P. Porous alumina templates and nanostructured CdS for thin film solar cell applications. *Solar Energy Mater Solar Cells* 2006;90 713–726.

[108] Kang Y, Kim D. Well-aligned CdS nanorod/conjugated polimer solar cells. *Solar Energy Mater Solar Cells* 2006;90 166–174.

[109] Nishizawa M, Mukai K, Kuwabata S, Martin CR, Yoneyama H, Nishizawa M, Mukai K, Kuwabata S, Martin CR, Yoneyama H. Template synthesis of polypyrrole-coated spinel $LiMn_2O_4$ nanotubules and their properties as cathode active materials for lithum batteries. *J Electrochem Soc* 1997;144 1923-1927.

[110] Chi GJ, Yao SW, Fan J, Zhang WG, Wang HZ. Antibacterial activity of anodized aluminium with deposited silver. *Surf Coat Technol* 2002;157 162–165.

[111] Choi J, Luo Y, Wehrspohn RB, Hillebrand R, Schilling J, Gosele U. Perfect two-dimensional porous alumina photonic crystals with duplex oxide layers. *J Appl Physics* 2003;94 4757-4762.

[112] Masuda H, Ohya M, Nishio H, Asoh H, Nakao M, Nohtomi M, Tamamura T. Photonic crystal using anodic porous alumina. *Jap J Appl Physics* 1999;38 L1403-L1405.

[113] Bocchetta P, Chiavarotti G, Masi R, Sunseri C, Di Quarto F. Nanoporous alumina membranes filled with solid acid for thin film fuel cells at intermediate temperatures. *Electrochem Commun* 2004;6 923-928.

[114] Librant K. Formation of porous alumina by anodic oxidation process in sulfosalicylic acid solution. MSc Thesis. Technical University of Warsaw; 2011, pp. 38.